INFECTION AND IMMUNITY, May 2008, p. 1979–1991 Vol. 76, No. 5
0019-9567/08/$08.00+0 doi:10.1128/IAI.01338-07

A Novel Sensor Kinase-Response Regulator Hybrid Controls Biofilm Formation and Type VI Secretion System Activity in *Burkholderia cenocepacia*▽

Daniel F. Aubert,[1] Ronald S. Flannagan,[1] and Miguel A. Valvano[1,2]*

Infectious Diseases Research Group, Departments of Microbiology and Immunology[1] and Medicine,[2] Siebens-Drake Research Institute, University of Western Ontario, London, Ontario, Canada

Received 4 October 2007/Returned for modification 14 November 2007/Accepted 15 February 2008

Burkholderia cenocepacia **is an important opportunistic pathogen causing serious chronic infections in patients with cystic fibrosis (CF). Adaptation of *B. cenocepacia* to the CF airways may play an important role in the persistence of the infection. We have identified a sensor kinase-response regulator (BCAM0379) named AtsR in *B. cenocepacia* K56-2 that shares 19% amino acid identity with RetS from *Pseudomonas aeruginosa*. *atsR* inactivation led to increased biofilm production and a hyperadherent phenotype in both abiotic surfaces and lung epithelial cells. Also, the *atsR* mutant overexpressed and hypersecreted an Hcp-like protein known to be specifically secreted by the type VI secretion system (T6SS) in other gram-negative bacteria. Amoeba plaque assays demonstrated that the *atsR* mutant was more resistant to *Dictyostelium* predation than the wild-type strain and that this phenomenon was T6SS dependent. Macrophage infection assays also demonstrated that the *atsR* mutant induces the formation of actin-mediated protrusions from macrophages that require a functional Hcp-like protein, suggesting that the T6SS is involved in actin rearrangements. Three *B. cenocepacia* transposon mutants that were found in a previous study to be impaired for survival in chronic lung infection model were mapped to the T6SS gene cluster, indicating that the T6SS is required for infection in vivo. Together, our data show that AtsR is involved in the regulation of genes required for virulence in *B. cenocepacia* K56-2, including genes encoding a T6SS.**

The *Burkholderia cepacia* complex (BCC) is a group of at least nine closely related gram-negative bacterial species. Ubiquitously present in the environment (3), BCC bacteria are also important opportunistic human pathogens that establish chronic lung infections in patients with chronic granulomatous disease and, most commonly, with cystic fibrosis (CF) (19). In some cases infection is further complicated by the "cepacia syndrome," which is characterized by an often fatal rapid lung deterioration, acute necrotizing pneumonia, and septicemia (24). BCC infections are of great concern to the CF community due to the intrinsic resistance of these bacteria to most clinically relevant antimicrobial agents (19) and their ability to be transmitted from person to person (18, 46). In most CF centers worldwide and more particularly in Canada, *B. cenocepacia* is the most common BCC species recovered from patients (42, 48) and is frequently associated with the most severe infections (31).

Adaptation of *B. cenocepacia* to the environment of the CF airways probably plays an important role in the establishment of a chronic infection. Sensing and adaptation to new environmental conditions by bacteria is commonly governed by two-component regulatory systems leading to modification of gene expression patterns required for bacterial survival (50). Two-component systems usually consist of a membrane-associated sensor (histidine kinase protein) that monitors environmental signals and a response regulator (receiver) whose function is modulated by phosphotransfer from its cognate histidine kinase (2, 55). Sensor histidine kinases respond to a wide range of signals, including those encountered during infection.

A global virulence regulator, PA4856 (RetS), has recently been identified in *Pseudomonas aeruginosa* (16). The *retS* gene encodes an unusual two-component regulator, containing a periplasmic sensor domain linked by a seven-transmembrane-spanning region to a histidine domain fused with two response regulator domains. RetS inversely controls the expression of genes associated with acute and chronic infections (16). Deletion of *retS* results in overexpression of two exopolysaccharide biosynthetic gene clusters (*pel* and *psl*), leading to a hyperadhesive phenotype on eukaryotic cell surfaces and increased biofilm production. Despite demonstrating strong adherence to eukaryotic cells, *P. aeruginosa retS* mutants do not respond to host cell contact, which normally activates the expression of genes encoding the type III secretion system (TTSS). Thus, *retS* mutants are not cytotoxic for tissue culture cells and are severely attenuated for virulence in an acute murine pneumonia model (16). Microarray analyses revealed that RetS is also involved in the downregulation of a virulence locus encoding a type VI secretion system (T6SS) (34).

The newly described T6SS is conserved in numerous gram-negative pathogens that interact closely with eukaryotic cells (8, 9, 41) and it has been recognized as an important contributor to pathogenesis in many bacteria (34, 40, 44, 51, 57). Little is known about the structure and organization of the T6SS apparatus, but several proteins specifically secreted by the T6SS have been identified. One such protein shares sequence similarity to the hemolysin-coregulated protein (Hcp) from *Vibrio cholerae* (56). Hcp appears to be secreted by most of the

* Corresponding author. Mailing address: Department of Microbiology and Immunology, Dental Sciences Building, Rm 3014, University of Western Ontario, London, Ontario, Canada N6A 5C1. Phone: (519) 661-3427. Fax: (519) 661-3499. E-mail: mvalvano@uwo.ca.

▽ Published ahead of print on 3 March 2008.

TABLE 1. Strains and plasmids

Strain or plasmid	Relevant characteristics[a]	Source and/or reference
B. cenocepacia strains		
K56-2	ET12 clone related to J2315, CF clinical isolate	BCRRC[b]; 30
DFA21	K56-2 *atsR*::pDA27; Tp^r	This study
DFA27	K56-2 Δ*hcp*	This study
DFA28	K56-2 Δ*hcp atsR*::pDA27; Tp^r	This study
E. coli strains		
DH5α	F^- Φ80d*lacZ*Δ*M15* Δ(*lacZYA-argF*)*U169 endA1 recA1 hsdR*17(r_K^- m_K^+) *supE44 thi-1* Δ*gyrA96 relA1*	Laboratory stock
SY327	*araD* Δ(*lac pro*) *argE*(Am) *recA56 nalA* λ *pir*; Rif^r	33
K. pneumoniae strain		
18		Laboratory stock
S. aureus strain		
RN6390		D. E. Heinrichs
Plasmids		
pME6000	ori_{pBBR1}, Tet^r, *lacZ, mob-*$^+$	S. Heeb
pMLS7-eGFP	ori_{pBBR1}, Tp^r, mob^+, P_{S7}	28
pGPΩTp	ori_{R6K}, ΩTp^r cassette, mob^+	14
pGPISce-I	ori_{R6K}, ΩTp^r , mob^+, containing the ISce-I restriction site	15
pAp2	ori_{pBBR1}, Cm^r, mob^+, P_{dhfr}	S. Cardona
pRK2013	$ori_{colE1,}$ RK2 derivative, Kan^r, mob^+, tra^+	13
pDA12	Cloning vector, ori_{pBBR1}, Tet^r, mob^+, P_{dhfr}	This study
pDA27	pGPΩTp; 272-bp internal fragment from *atsR*	This study
pAtsR	pDA12; 1.8-kbp *atsR* fragment	This study
pDA42	pDA12; 0.7-kbp *eGFP* fragment	This study
pDA45	pGPISce-I with fragments flanking *hcp*	This study
pHcp	pDA12; 0.5-kbp fragment encoding Hcp	This study
pDAISce-I	pDA12 encoding the ISce-I homing endonuclease	15

[a] Tp^r, trimethoprim resistance; Cm^r, chloramphenicol resistance; Kan^r, kanamycin resistance; Tet^r, tetracycline resistance; Rif^r, rifampin resistance.
[b] BCRRC, *B. cepacia* Research and Referral Repository for Canadian CF Clinics.

T6SSs studied to date, and secretion of Hcp is the hallmark of a functional T6SS in many bacterial species (39). The function of Hcp-like proteins remains unknown. In *Aeromonas hydrophila*, Hcp is translocated into eukaryotic cells via the T6SS, and Hcp expression in transfected HeLa cells can induce apoptosis (51). In *V. cholerae*, Hcp is not cytotoxic by itself but is required for the extracellular secretion of three other proteins, namely, VgrG-1, VgrG-2, and VgrG-3 (40). The function of these proteins is also unknown, but VgrG-1 shares a subdomain with the *V. cholerae* RtxA toxin that mediates covalent actin cross-linking (39, 45). Recently, the crystal structure of the *P. aeruginosa* Hcp1 protein was determined (34). Hcp1 forms a hexameric ring with a large internal diameter, and it was hypothesized that Hcp1 may also participate as a structural scaffold in the secretion of other substrates. Protein structure search algorithms predicted that VgrG-related proteins likely assemble into a trimeric complex that is analogous to the baseplate "tail-spike" of bacteriophage T4 (39), differentiating the T6SS from other canonical secretion systems.

We report here the identification of AtsR (adherence and T6SS regulator), a putative sensor kinase hybrid homologous to RetS that controls the expression of *hcp* and biofilm formation in *B. cenocepacia* K56-2. Experiments employing amoeba plaque assays and macrophage infection assays demonstrate that an *atsR* mutant of *B. cenocepacia* K56-2 utilizes the T6SS to interact with eukaryotic cells. This study describes for the first time the presence of a functional T6SS in *B. cenocepacia* K56-2 and its importance for the virulence of this bacterium.

MATERIALS AND METHODS

Bacterial strains, plasmids, and culture media. Bacterial strains and plasmids used in this study are listed in Table 1. Bacteria were cultured in Luria broth (LB) (Difco) at 37°C with shaking. *Escherichia coli* cultures were supplemented as required with the following antibiotics (final concentrations): tetracycline (30 μg ml^{-1}), kanamycin (30 μg ml^{-1}), trimethoprim (50 μg ml^{-1}), and gentamicin (50 μg ml^{-1}). *B. cenocepacia* cultures were supplemented as required with trimethoprim (100 μg ml^{-1}), tetracycline (100 μg ml^{-1}), and gentamicin (50 μg ml^{-1}). To assess the growth rates of parental and mutant strains of *B. cenocepacia* K56-2, overnight cultures were inoculated into fresh medium with a starting optical density at 600 nm (OD_{600}) of 0.05. Growth rates were determined in 100-well microtiter plates by use of a Bioscreen C automated microbiology growth curve analysis system (MTX Lab Systems, Inc., Vienna, VA) under high-amplitude shaking conditions.

General molecular techniques. DNA manipulations were performed as described previously (43). T4 polynucleotide kinase and T4 DNA ligase (Roche Diagnostics, Laval, Quebec, Canada) were used as recommended by the manufacturers. Transformation of *E. coli* DH5α was done by the calcium chloride protocol (4). *E. coli* SY327 carrying the helper plasmid pRK2013 (13) was transformed by electroporation (11), and the transformants were used as donors for conjugation into *B. cenocepacia* K56-2. DNA amplification by PCR was performed using a PTC-221 DNA engine (MJ Research, Incline Village, NV) with either *Taq* DNA polymerase or proof start polymerase (Qiagen Inc., Mississauga, Ontario, Canada). DNA sequencing was performed by the Robarts Research Institute DNA sequencing facility at the University of Western Ontario, London, Canada.

TABLE 2. Oligonucleotide primers

Primer no.	5′–3′ primer sequence[a]	Restriction enzyme[b]
1548	GAGCTCATCGATTTCGTTCCACTGA	ClaI
1549	TCATCGATCTGCACTTGAACGTGTGGCC	ClaI
2143	AGTCGAAGGCATATGTTACACATGCACTTGCAG	NdeI
2165	TAATCGATGGCTCTGCTGTAGTGAGTGG	ClaI
2166	CGATCGATGCGAAGAAGTTGTCCATATTG	ClaI
2478	TTTTTCTAGAGTCAACGAGGGCGTGCTC	XbaI
2479	CCGTCATGAATTCGCCCAGCGC	EcoRI
2558	TTTTCATATGCCGCTCGGCGAAGCCAAGT	NdeI
2559	GTTTTCTAGATCAGGCGAGCAGTGTCTCGA	XbaI
2780	GTGTTCTAGACCGTCGAATACGCGAAGTG	XbaI
2781	GCGGCTCGAGCAAACTGCAAGTGCAT	XhoI
2782	TTTTCTCGAGACGACAAGACCTACG	XhoI
2783	GGTGAATTCGGGGTAGTCGTC	EcoRI
2798	GCAGCCAGTATTGGGACACT	N/A
2799	TGCATCGACGAATACACGTT	N/A
2805	GACGTGACGATCGTATGCTG	N/A
2806	ATGGCTACATCCTCGACTGG	N/A
2943	ATGATCTAGATTAGACCGCGTAGGTCTTGTCGT	XbaI
3143	AGCTGGCAGTACACGGAAAG	N/A
3136	GCACGACCATCACGATCTC	N/A
3315	ACGTTCTCGCTGAAGTACGC	N/A
3318	CGCGTAGGTCTTGTCGTTCT	N/A

[a] Restriction endonuclease sites incorporated in the oligonucleotide sequences are underlined.
[b] N/A indicates the absence of restriction site.

RT-PCR and quantitative RT-PCR reactions. Reverse transcriptase PCR (RT-PCR) was performed as described previously (36) to investigate the transcriptional organization of *atsR* (BCAM0379) and the neighboring genes BCAM0380 and BCAM0381. Total RNA was isolated from *B. cenocepacia* K56-2 by use of the RNeasy mini kit (Qiagen) following the manufacturer's protocol and treated with DNase (Qiagen) for 30 min at 37°C and at 75°C for 15 min. Reverse-transcribed cDNAs were amplified using primers 2798 and 2805 (Table 2). Each reverse transcription reaction was performed with RT and without RT (negative control). PCR amplifications with primer pairs 2798-2799 and 2805-2806 were performed using the cDNAs and *B. cenocepacia* K56-2 genomic DNA (positive control) as the template to amplify the intergenic regions of *atsR*-BCAM0380 and BCAM0380-BCAM0381, respectively.

Quantitative real-time PCR experiments were performed as follows. Overnight cultures grown at 37°C for 16 h were diluted to an OD_{600} of 0.05 in 30 ml of prewarmed LB. Diluted cultures of *B. cenocepacia* K56-2 and the K56-2 *atsR*::pDA27 mutant, DFA21, were grown at 37°C until exponential phase, harvested, and used for RNA extraction. Total RNA was isolated using a RiboPure-Bacteria kit (Ambion, Austin, TX), according to the manufacturer's instructions. RNA samples were treated with 8 U of DNaseI, which was inactivated using DNase inactivation reagent (Ambion, Austin, TX). The concentration of RNA samples was measured using a NanoDrop ND-1000 spectrophotometer (Thermo Fisher Scientific, Wilmington, DE). The histidinol dehydrogenase gene *hisD* (BCAL0312), which is involved in histidine biosynthesis, was used as a reference standard. The cDNAs from *hisD* and *hcp* were generated using the reverse gene-specific primers 3136 and 3318, respectively (Table 2). Reverse transcription reactions were performed in 20-μl mixtures (1× RT buffer, 2 μM *hisD* reverse primer [3136], 2 μM *hcp* reverse primer [3318], deoxynucleoside triphosphate at a concentration of 1 mM, 1 U/μl RNase inhibitor, 1 μg of total RNA template). The reverse transcription reactions were performed with 0.75 U/μl of RT and without RT (negative control). To construct standard curves for quantification, PCR products corresponding to internal fragments of *hisD* and *hcp* were amplified using primers 3143-3136 and 3315-3318, respectively (Table 2). The PCR products were purified and the concentration was measured using a NanoDrop ND-1000 spectrophotometer. The number of copies per microliter of each product was calculated and dilutions were performed to obtain solutions with a final concentration of 5.10^5 copies/μl. Then, 10-fold dilutions were performed up to a concentration of 5 copies/μl. Two microliters of each dilution or cDNA was subjected to real-time PCR using iQ SYBR green supermix (Bio-Rad) along with the primer pair 3143-3136 for *hisD* and the primer pair 3315-3318 for *hcp*. mRNA expression levels of *hisD* and *hcp* in the *B. cenocepacia* K56-2 and DFA21 strains were quantified on a Rotor-Gene 6000 quantitative multiplex PCR instrument (Corbett, Sydney, Australia) with the following parameters: 95°C for 3 min, followed by 40 PCR cycles consisting of 95°C for 10 s, 55°C for 15 s, and 72°C for 30 s. The concentrations of *hcp* mRNA in samples were normalized to concentrations of *hisD* mRNA. The experiment was repeated three times.

Construction of pDA12 and pDA42. The plasmid pDA12 is a derivative of pAP2 (a pMLBAD derivative [28] containing the *dhfr* promoter and a *cat* gene; from S. Cardona, unpublished) in which the chloramphenicol resistance cassette has been replaced by a tetracycline resistance cassette as follows. The *tetA* and *tetR* genes were PCR amplified from pME6000 by use of the primers 2165 and 2166, which contain a ClaI restriction site at their 5′ ends (Table 2). The backbone of the pAP2 plasmid was PCR amplified using the Expand high-fidelity PCR system (Roche Diagnostics) and the primer pair 1548 and 1549, which also contained a ClaI restriction site. The resulting amplicons were digested with ClaI and ligated, giving rise to pDA12 (Table 1). The gene encoding the enhanced green fluorescent protein (eGFP) was excised from pMLS7-eGFP and subcloned into pDA12 by use of the restriction enzymes HindIII and EcoRI (Table 1). The resulting plasmid, pDA42, was introduced into *B. cenocepacia* K56-2 and DFA21 by conjugation, and expression of the eGFP was confirmed by fluorescence microscopy.

Mutagenesis of *B. cenocepacia* K56-2. Insertional inactivation of *B. cenocepacia* K56-2 genes was performed using pGPΩTp, a suicide plasmid encoding resistance to trimethoprim (14). This plasmid is derived from the pGP704 backbone, which carries the Pir protein-dependent R6K origin of replication (25). The sensor kinase regulator gene *atsR* was mutated by first PCR amplifying a 272-bp internal fragment from *B. cenocepacia* K56-2 chromosomal DNA by use of the primer pair 2478 and 2479 (Table 2). The PCR cycling conditions used were as follows: 95°C for 5 min followed by 30 cycles of 95°C for 45 s, 60°C for 45 s, and 72°C for 30 s, with a final extension at 72°C for 5 min. The resulting amplicon was digested with the restriction enzymes EcoRI and XbaI and cloned into similarly digested pGPΩTp. The resulting plasmid, pDA27, was introduced into *B. cenocepacia* K56-2 by conjugation, and the resulting exconjugants were selected for resistance to trimethoprim. Candidate mutants were identified by PCR and confirmed by Southern blot hybridization using the internal fragment labeled with digoxigenin as a probe. The resulting mutant was named *B. cenocepacia* DFA21 (Table 1).

Deletion of *hcp* (BCAL0343) encoding an Hcp-like protein (*B. cenocepacia* K56-2 Δ*hcp*; strain DFA27) was performed using a recently developed system based on the I-SceI homing endonuclease (15). Briefly, this system allows the creation of unmarked and nonpolar mutations and comprises two plasmids. One plasmid, pGPISce-I, serves to clone the regions flanking the gene to be deleted and contains a restriction site for a homing endonuclease. Once introduced by conjugation, the mutagenic plasmid integrates into the *B. cenocepacia* K56-2

chromosome, giving rise to trimethoprim-resistant mutants. A second plasmid, pDAISce-I (pDA12 derivative encoding the I-SceI endonuclease), is introduced by conjugation. Homing endonucleases catalyze site-specific double-strand breaks in the chromosome at the recognition site. As DNA double-strand breaks are lethal, only mutants undergoing second homologous recombination events, including those with a deletion of the gene of interest, can be recovered. PCR amplifications of regions flanking *hcp* were performed using 2780-2781 and 2782-2783 primer pairs (Table 2). The amplicons were digested with the restriction enzymes XbaI-XhoI and XhoI-EcoRI, respectively, and cloned into pGPISce-I digested with EcoRI and XbaI, giving rise to pDA45. The resulting mutant was designated DFA27 (Table 1). Deletion of *hcp* was also performed in combination with *atsR* inactivation, giving rise to *B. cenocepacia* DFA28 (the *atsR*::pDA27 Δ*hcp* mutant). The deletion of *hcp* was first analyzed by PCR and then confirmed by Southern blot hybridization.

Complementation experiments. To complement *B. cenocepacia* DFA21, wild-type *atsR* was PCR amplified from *B. cenocepacia* K56-2 with the primer pair 2558 and 2559 with the following thermal cycling conditions: 95°C for 5 min followed by 30 cycles of 95°C for 45 s, 60°C for 45 s, and 72°C for 2 min, with a final extension at 72°C for 10 min. The resulting amplicon was digested with the restriction enzymes NdeI and XbaI and ligated into similarly digested pDA12. The resulting plasmid, pAtsR, was introduced into the mutant by conjugation, and complementation was assessed by the biofilm assay. To complement DFA27 (Δ*hcp*) and DFA28, *hcp* was PCR amplified using primers 2143 and 2943 cloned as an NdeI and XbaI fragment in pDA12 as indicated above, giving rise to pHcp.

Biofilm formation. In a modification of the biofilm ring assay (37), overnight cultures grown at 37°C for 16 h were diluted to an OD_{600} of 0.005 in LB, and triplicate 500-μl aliquots were dispended into polystyrene tubes. Following 24 h of static incubation at 37°C, the medium was removed and the tubes were washed gently with distilled water. Adherent bacteria were stained with 1% (wt/vol) crystal violet and washed three times with distilled water. The bound crystal violet was dissolved in 1 ml of 100% methanol and quantified by measuring the absorbance at 540 nm. The experiment was repeated independently three times.

Adherence assays. Abiotic adherence assays were performed as follows. Bacteria grown in LB at 37°C for 21 h were washed twice and resuspended in phosphate-buffered saline (PBS; Wisent). Approximately 10^7 CFU were added in duplicate to the wells of a six-well polystyrene plate (BD Biosciences, Mississauga, Ontario, Canada) containing 2 ml of PBS. Additionally, serial 10-fold dilutions were performed on the starting inoculum, and 100 μl of each dilution was plated on LB agar plates to determine precisely the number of bacteria added to each well (input). The six-well plates were centrifuged for 2 min at 300 × *g* and incubated at 37°C for 10 min. Each well was washed five times with 2 ml of PBS, and bound bacteria were detached from the surface with the addition of 500 μl of 10 mM EDTA and 1.5 ml of 1% (vol/vol) Triton X-100. Bacteria were then centrifuged at 4,500 × *g* for 4 min, and the pellet was resuspended in 1 ml PBS. Serial 10-fold dilutions were performed and 100 μl of each dilution was plated on LB agar plates and incubated at 37°C. The colony enumeration was performed the following day to determine the number of bacteria that remained adherent to the six-well plate after the PBS washes (output). The adherence of each strain tested was calculated by dividing the output number by the input number and expressed relative to the adherence of *B. cenocepacia* K56-2 wild type, which was set as 1. The experiment was repeated independently three times.

A549 lung epithelial cell adherence assays were performed with *B. cenocepacia* K56-2 and DFA21 carrying pDA42 (expressing eGFP) to facilitate bacterial numeration as follows. Bacterial cultures grown at 37°C for 21 h were washed twice and resuspended in RPMI 1640 (Wisent). Bacteria were added at a starting multiplicity of infection (MOI) of 100:1 in triplicate to A549 cells grown on glass coverslips in six-well tissue culture plates containing 2 ml of Dulbecco's modified Eagle medium (DMEM) with 10% (vol/vol) fetal bovine serum (FBS). No centrifugation was performed, and the plates were incubated at 37°C in a humidified atmosphere of 95% and 5% carbon dioxide (CO_2). After 1 h, wells were gently washed five times with 2 ml of RPMI 1640 to remove nonadherent bacteria, and 4′,6′-diamidino-2-phenylindole dihydrochloride (DAPI) (final concentration, 25 μg/ml; Molecular Probes, Invitrogen, Eugene, OR) was added to visualize eukaryotic cell nuclei. The total number of cell-attached bacteria and the total number of cells were counted in 21 fields of view. The experiment was repeated independently three times.

Preparation of culture supernatant proteins and mass spectrometry. Overnight cultures were diluted to an OD_{600} of 0.003 in 50 ml of prewarmed LB. After 4 h of incubation at 37°C, the cultures were centrifuged for 15 min at 10,000 × *g* at 4°C. Culture supernatants were sterilized through a 0.22-μm filter (Millipore), and proteins were precipitated overnight at 4°C with 10% (vol/vol) of trichloroacetic acid (final concentration). The precipitates were isolated by centrifugation at 10,000 × *g* for 20 min at 4°C and the pellets were washed with ice-cold acetone. Another centrifugation was performed at 10,000 × *g* for 20 min. The pellets were air dried and then resolubilized by the addition of 0.1 M sodium phosphate buffer, pH 7.0. The protein concentration of each sample was determined by Bradford assay (Bio-Rad), and aliquots containing 10 μg of protein were loaded on a 16% sodium dodecyl sulfate-polyacrylamide electrophoresis (SDS-PAGE) gel. Detection was performed with a Brilliant Blue G-Colloidal staining according to the manufacturer's recommendations (Sigma, St. Louis, MO).

The apparent 21-kDa protein band was excised from a Brilliant Blue G-Colloidal-stained one-dimensional gel loaded with 20 μg of secreted proteins from *B. cenocepacia* DFA21 by use of an Ettan spot picker (Amersham). In-gel trypsin digestion was performed by the Functional Proteomics Facility of the University of Western Ontario using the Waters MassPREP automated station. Mass spectrometry analysis was performed by the Biological Mass Spectrometry Laboratory of the University of Western Ontario on a Micromass Q-Tof global mass spectrometer equipped with a Z-spray source operating in the positive-ion mode. A 1-hour gradient was used on a C_{18} column fitted with a trapping column by use of the Waters Nano Acquity UPLC instrument. Data were acquired using MassLynx 4.1 and were submitted for screening via the MASCOT search engine (Matrix Science, London, United Kingdom).

***Dictyostelium discoideum* plaque assay.** *D. discoideum* axenic strain AX3 was obtained from the Dicty Stock Center (Columbia University) and grown in HL5 liquid medium at 22°C according to the Dictybase guidelines (http://www.dictybase.org/). *D. discoideum* cells from mid-log-phase cultures were collected by centrifugation (100 × *g*, 3 min), washed once, and resuspended in SorC (16.7 mM Na_2H-KH_2PO_4–50 μM $CaCl_2$, pH 6.0) (52). Bacteria were grown in LB for 16 h, pelleted by centrifugation, washed once, and resuspended in SorC. The growth of *D. discoideum* on a lawn of *B. cenocepacia* K56-2 cells was determined by plating 100 μl of a suspension containing ~100 amoebae and 10^7 CFU on SM agar or on low-nutrient plates, SM/50 and SM/100, which contained 1/50 and 1/100 of the SM stock solution, respectively (52). Quantitative measurements of *D. discoideum* growth on a lawn of *B. cenocepacia* cells were obtained by first plating 200 μl of a bacterial suspension at 10^9 CFU/ml on SM agar. Then, the bacterial lawn was spotted with 5-μl droplets containing serial dilutions of *D. discoideum*. Plates were incubated at 22°C for 3 days and examined for plaque formation by *D. discoideum*. *Klebsiella pneumoniae* 18 was used as a positive control for predation by *D. discoideum*.

***D. discoideum* cytotoxicity assay.** *D. discoideum* cells were prepared as described above. *K. pneumoniae* 18, *Staphylococcus aureus* RN6390, and K56-2(pDA12) and DFA21(pDA12) cultures were grown in 5-ml portions of HL5 medium at 37°C for 16 h. The bacteria were pelleted by centrifugation, and culture supernatants were collected and filtered (0.22-μm filter pore size). One milliliter of supernatant was incubated with approximately 500 amoebae and mixed by inversion at room temperature for 1 h. The effect of bacterial culture supernatants on *D. discoideum* growth was determined by plating 200 μl of the amoebal suspension on SM agar plates on which 200 μl of a bacterial suspension at 10^9 CFU/ml of *K. pneumoniae* was previously dispersed. Plates were incubated at 22°C for 5 days and examined for plaque formation by *D. discoideum*. HL5 medium and *S. aureus* RN6390 were used as negative and positive controls of cytotoxicity toward *D. discoideum*, respectively.

Macrophage infection assays and immunofluorescence microscopy. The C57BL/6 murine bone marrow-derived macrophage cell line ANA-1 was obtained from the Department of Human Genetics, Montreal General Hospital Research Institute, McGill University, Montreal, Quebec, Canada (7). Cells were maintained in DMEM with 10% FBS and grown at 37°C in a humidified atmosphere with 5% CO_2. One milliliter of bacterial cultures grown at 37°C for 16 h was washed twice and resuspended in DMEM-10% FBS. Heat-inactivated bacteria were obtained by incubation at 60°C for 25 min prior to infection. Bacteria were added to ANA-1 cells grown on glass coverslips at a MOI of 50:1 and centrifuged for 1 min at 300 × *g*. After 4 h of incubation at 37°C, infected macrophages were washed three times with 2 ml of DMEM and the coverslips were analyzed immediately or used for immunostaining as follows. Cells were fixed in 4% paraformaldehyde (vol/vol) for 30 min at room temperature and incubated for 10 min with 100 mM glycine in PBS (1×). Cells were then permeabilized with 0.1% Triton X-100 (vol/vol) and blocked with 5% milk powder (wt/vol) for 1 h at room temperature. Permeabilized cells were incubated with primary antibodies followed by secondary antibodies in 5% milk powder for 1 h each at room temperature. Coverslips were mounted onto glass slides by use of fluorescent mounting medium (DakoCytomation). Rabbit anti-*B. cenocepacia* K56-2 primary antibody was used at a dilution of 1:500, and the Alexa Fluor 647 goat anti-rabbit immunoglobulin G secondary antibody (Molecular Probes, Invitrogen) was used at a dilution of 1:1,000. For fluorescence labeling of actin,

macrophages were incubated with one unit of Alexa Fluor 488 phalloidin (Molecular Probes, Invitrogen). Fluorescence and phase-contrast images were acquired using a Qimaging (Burnaby, British Columbia, Canada) cooled charge-coupled-device camera on an Axioscope 2 (Carl Zeiss, Thornwood, NY) microscope with an X100/1.3 numerical aperture Plan-Neofluor objective and a 50-W mercury arc lamp. Images were digitally processed using the Northern Eclipse version 6.0 imaging analysis software (Empix Imaging, Mississauga, Ontario, Canada). Confocal microscopy was performed using a Zeiss LSM 510 META/ConfoCor2 laser scanning confocal microscope and a 100× oil immersion objective. Bacterially induced cell death or damage was verified by using trypan blue staining (Sigma) (final concentration, 1 mg/ml) for 10 min.

RESULTS

AtsR regulates biofilm formation in *B. cenocepacia* K56-2. We examined the sequenced genome of *B. cenocepacia* J2315, which is clonally related to K56-2 (30), to identify genes encoding a homolog of *P. aeruginosa* RetS (PA4856) (16). BLASTP analysis (http://www.ncbi.nlm.nih.gov/BLAST/) allowed the identification of several genes encoding RetS-like putative response regulators: BCAM0227, BCAM0379, BCAM1505, and BCAM2757. Mutations in each of these putative response regulators were generated by insertional inactivation using the plasmid pGPΩTp, a mutagenesis system leading to the targeted insertion of a mutagenesis plasmid (14, 29). Since *retS* inactivation in *P. aeruginosa* leads to increased biofilm production (16), our insertional mutants were screened for biofilm formation. BCAM0227, BCAM1505, and BCAM2757 insertional mutants did not have an apparent biofilm defect in vitro (data not shown). The BCAM0379 insertional mutant formed a strong biofilm ring after 24 h of static incubation (Fig. 1A). For reasons discussed below, we have assigned to BCAM0379 the name *atsR* (*a*dherence and *T*6SS *r*egulator). Quantitation of the biofilm mass demonstrated that the *atsR*::pDA27 mutant, DFA21, produced 50% more biofilm than the wild-type strain ($P = 0.0001$) (Fig. 1B). Growth curves of wild-type K56-2 and DFA21 in liquid media were similar, suggesting that increased biofilm formation by DFA21 was not due to faster growth (data not shown). *Trans*-complementation of DFA21 with pAtsR, encoding only AtsR, restored biofilm formation to parental levels (Fig. 1A and B) and also confirmed that the insertion into *atsR* did not affect the neighboring genes. Moreover, the overexpression of *atsR* in the wild-type strain, K56-2, led to decreased biofilm formation (data not shown). Together, these results suggest that AtsR acts as a negative regulator of biofilm formation.

The *atsR* gene is on chromosome 2 and encodes a predicted 606-amino-acid protein that belongs to the sensor kinase-response regulator hybrid family but shares only 19% identity at the primary amino acid sequence with RetS (16). Analysis using SignalP 3.0 (http://www.cbs.dtu.dk/services/SignalP/) and TMHMM (http://www.cbs.dtu.dk/services/TMHMM-2.0/) predicted a signal peptide sequence and one transmembrane domain at the N terminus, suggesting that AtsR is inserted in the inner membrane. Predicted histidine kinase and ATPase domains following the transmembrane domain were detected using Pfam (http://pfam.sanger.ac.uk/) (1). Unlike RetS, the C terminus of AtsR contains only one predicted response regulator-like receiver domain. However, similar to RetS, AtsR lacks the DNA binding domain characteristic of conventional response regulator proteins, suggesting that AtsR is a component of a multipart signaling pathway. Comparisons with sequences deposited in GenBank showed that AtsR is conserved among the *Burkholderia* genus. Homologs sharing 95%, 86%, 84%, 66%, and 65% amino acid identity with AtsR from *B. cenocepacia* are found in *B. ambifaria*, *B. cepacia*, *B. vietnamiensis*, *B. thailandensis*, and *B. pseudomallei* species, respectively.

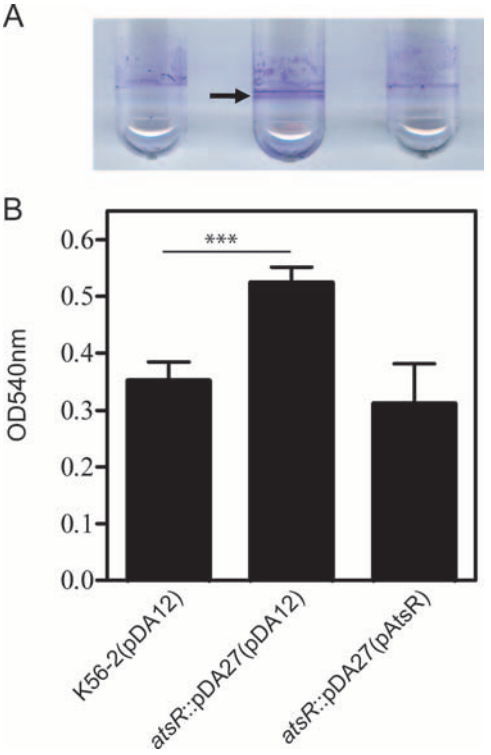

FIG. 1. Biofilm assays performed with *B. cenocepacia* K56-2 (wild type [WT]) and DFA21 (the *atsR*::pDA27 mutant) containing the control plasmid pDA12 or pAtsR, as indicated in parentheses. Biofilms were quantified by crystal violet staining after 24 h of static incubation at 37°C. (A) The ring corresponding to robust biofilm formation characteristic of the *atsR* mutant is indicated by an arrow. (B) The extent of crystal violet retention by adherent bacteria was measured by OD_{540}. Data shown are the means of three independent experiments done in triplicate. Error bars represent the standard deviations. Significant differences were determined using unpaired *t* tests. The three asterisks indicate that the *P* value is 0.0001.

Two genes are located upstream of *atsR* and in the same transcriptional orientation (Fig. 2A): (i) BCAM0380, encoding a putative periplasmic protein of unknown function containing an oxidoreductase molybdopterin binding domain; and (ii) BCAM0381, encoding a putative cytoplasmic transcriptional regulator containing an N-terminal BetR helix-turn-helix domain and a response regulator domain at the C terminus. RT-PCR experiments performed on the intergenic regions of BCAM0381-BCAM0380 and BCAM0380-*atsR* revealed that these three genes are cotranscribed (Fig. 2B).

Mutation in *atsR* induces a hyperadhesive phenotype. As surface attachment is the first step in biofilm formation, *B. cenocepacia* DFA21 was tested for adherence on abiotic surfaces by use of an assay that measures the strength of bacterial adhesion after extensive washes with buffer and that also allows a comparison of the adherence levels of different strains within the same six-well plate (see Materials and Methods). For a given strain, the ratio of output to input bacteria can vary from

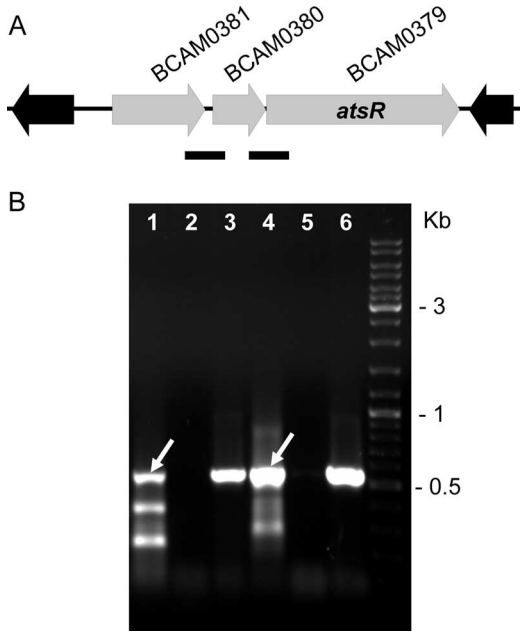

FIG. 2. Genetic organization and analysis of the gene cluster encoding AtsR in *B. cenocepacia* J2315 and K56-2. The direction of transcription of each gene is denoted by gray arrows. BCAM gene designations are according to a preliminary annotation of the *B. cenocepacia* J2315 genome (http://www.sanger.ac.uk/Projects/B_cenocepacia/). (A) Three-gene cluster located on chromosome 2 comprising BCAM0379 (*atsR*), BCAM0380, and BCAM0381. Black arrows represent genes located at the boundaries of the three-gene cluster containing *atsR*. Solid black bars indicate the regions analyzed by RT-PCR shown in panel B. (B) RT-PCR analysis of the intergenic regions of BCAM0381-BCAM 0380 and BCAM0380-*atsR*. Lanes: 1 to 3, RT, no RT, and DNA for BCAM0381-BCAM0380; 4 to 6, RT, no RT, and DNA for BCAM0380-*atsR*. White arrows indicate bands of expected PCR product size.

experiment to experiment because of fluctuations in the manual washing procedure. However, the relative adherence of the strains examined in the same plate, compared to that of the wild type in the control well, is conserved between experiments. This adhesion assay revealed that DFA21 is 100-fold more adherent than the wild-type strain, whose adhesion properties allows the adherence of approximately 0.1% of the starting inoculum. As expected, complementation of DFA21 with pAtsR decreased adherence to wild-type levels (Fig. 3A). To determine whether DFA21 displayed similar hyperadhesive properties to human cells, A549 lung epithelial cells were incubated with DFA21 or the wild-type strain. After only 1 h of incubation, DFA21 exhibited a sixfold-increased adherence ($P = 0.0002$) compared to the parental strain (Fig. 3B and C). Together, these results suggest that the *atsR*::pDA27 mutant, DFA21, is more adherent than the wild-type strain to both abiotic surfaces and lung epithelial cells.

Mutation in *atsR* increases expression and secretion of an Hcp-like protein. SDS-PAGE analysis of concentrated culture supernatants revealed a small protein with an apparent mass of ~21 kDa that was hypersecreted by DFA21 compared to what was seen for the wild type (Fig. 4). DFA21 carrying pAtsR also secreted the 21-kDa protein, albeit at an intermediate level compared to that of wild-type K56-2(pDA12) and DFA21 (pDA12). The apparent mass of the secreted protein, together with the RetS-like properties of AtsR, led us to hypothesize that the 21-kDa polypeptide is an Hcp-like protein. Hcp-like proteins are specifically secreted by the T6SSs of several gram-negative bacteria (34, 40, 44), and Hcp secretion is the hallmark of a functional T6SS activity in many bacterial species (39). In-gel trypsin digestion and mass spectrometry were performed on the 21-kDa protein. Acquired data were submitted for screening via the MASCOT search engine and two peptides were identified, matching with a score of 121 to DUF796, a protein of unknown function corresponding to Hcp.

In a previous study, we identified transposon insertions in-

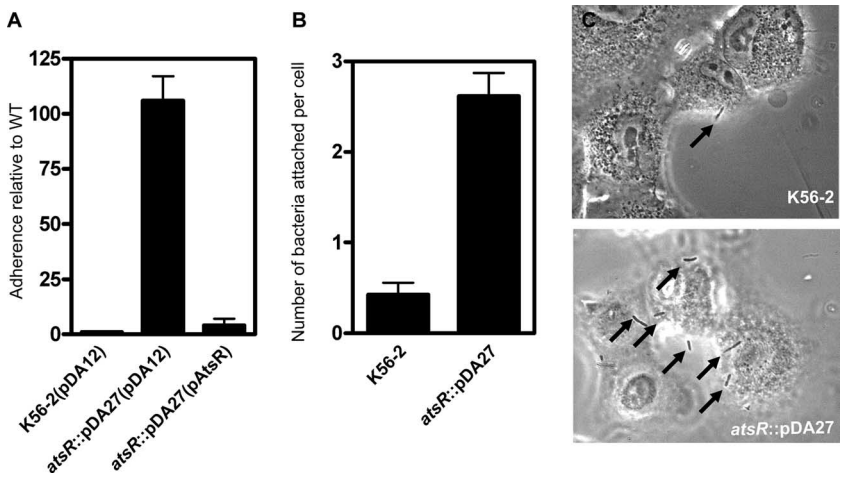

FIG. 3. Adhesion assays. (A) Adhesion assay to a polystyrene surface of bacterial strains with the control vector pDA12 and the pAtsR plasmids, as indicated in parentheses. *atsR* indicates the DFA21 mutant. The adhesion values are shown relative to the value for the control strain, *B. cenocepacia* K56-2(pDA12), which was set as 1. (B) Adhesion assay on A549 human lung epithelial cells. A549 cells were incubated with *B. cenocepacia* K56-2 and *B. cenocepacia* DFA21 (indicated by *atsR*) for 1 h at 37°C, washed, and stained, and the adherent bacteria were enumerated. Data shown are the means of three independent experiments. Error bars represent the standard deviations. (C) Representative images of A549 cell adherence by *B. cenocepacia* K56-2 and *B. cenocepacia* DFA21 (*atsR*) are shown. Arrows point to adherent bacteria. WT, wild type.

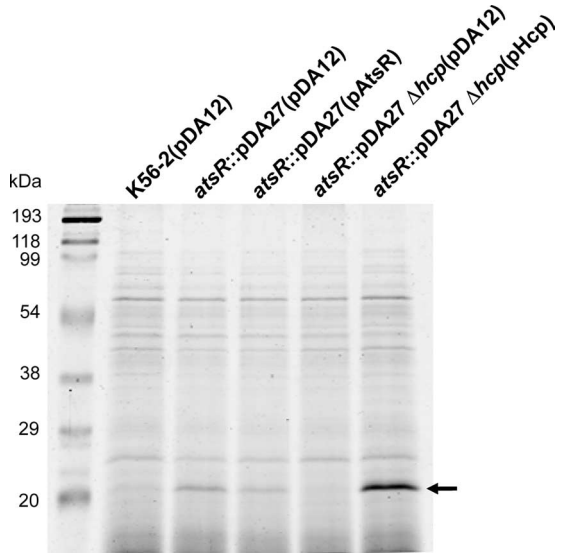

FIG. 4. Secretion assay. SDS-PAGE analysis of concentrated culture supernatants recovered from strains containing the control plasmid pDA12 or the plasmids pAtsR and pHcp, as indicated in parentheses. *atsR* indicates DFA21; *atsR* Δ*hcp* indicates DFA28. Molecular mass markers in kDa are also indicated. The arrow points to the secreted Hcp polypeptide analysis of concentrated culture supernatants recovered from strains containing the control plasmid pDA12 or the plasmids pAtsR and pHcp, as indicated in parentheses. Molecular mass markers in kDa are also indicated. The arrow points to the position of secreted Hcp polypeptide. WT, wild type.

activating genes that abolish the infectivity of *B. cenocepacia* K56-2 in the rat agar bead model of chronic lung infection (22). Further analysis revealed that three of these mutants (1A5, 34C4, and 34C6) had insertions that mapped within genes now referred to as *bcsA*, *bcsF* (*clpV*), and *bcsO*, which are part of a T6SS gene cluster (Fig. 5). In contrast to other *Burkholderia* species (44), *B. cenocepacia* K56-2 contains only one T6SS gene cluster located on chromosome 1, comprising genes organized in three putative transcriptional units (Fig. 5). BCAL0343, located within this cluster, encodes a 167-amino-acid protein orthologous to the Hcp-like proteins secreted by *P. aeruginosa* (PA0085) and *V. cholerae* (VCA0017) and has a predicted molecular mass of 18.4 kDa. Similar to other Hcp-like proteins, *B. cenocepacia* Hcp (BCAL0343) lacks a canonical hydrophobic amino-terminal signal sequence.

To confirm that the secreted 21-kDa protein is encoded by *hcp*, we constructed DFA28 carrying a deletion of *hcp* in combination with an insertional mutation in *atsR*. The 21-kDa protein was absent from the concentrated supernatant of the double mutant, DFA28, but its secretion was restored by introducing pHcp, which constitutively expresses Hcp (Fig. 4). We conclude that mutation of *atsR* leads to hypersecretion of Hcp. To determine whether *hcp* expression is upregulated in DFA21, quantitative real-time PCR experiments were performed. mRNA expression levels for *hcp* in the *B. cenocepacia* K56-2 and DFA21 strains were quantified and normalized to mRNA expression of *hisD*, which was used as the standard. The expression ratio of DFA21 to the wild type was greater than 5, confirming that the mutation of *atsR* resulted in an increase of *hcp* expression compared to what was seen for wild-type K56-2. Since Hcp secretion is indicative of T6SS activity (39), our results suggest that the T6SS is upregulated in DFA21.

Mutation in *atsR* increases T6SS-dependent growth inhibition of *Dictyostelium discoideum* by *B. cenocepacia*. Virulence of DFA21 was assessed using the social amoeba *D. discoideum*, a model host that preys on bacteria through its phagocytic feeding behavior. Several pathogenic bacteria resist *Dictyostelium* predation by producing factors that either actively kill the amoebae (6, 38) or allow intracellular survival and bacterial replication (20, 47). *D. discoideum* is remarkably similar to mammalian macrophages and infection assays performed with *P. aeruginosa*, *Legionella pneumophila*, and *Mycobacterium* species revealed that the same virulence mechanisms implicated in resistance to *Dictyostelium* predation also operated against mammalian cells (6, 49).

The susceptibility of *B. cenocepacia* K56-2 to *D. discoideum* predation was first tested using a qualitative plaque assay. *D. discoideum* cells were mixed with either *B. cenocepacia* K56-2 or *K. pneumoniae* 18, a strain known to be permissive for *D. discoideum* growth, and plated on SM agar plates. After a few days, *K. pneumoniae* was successfully killed by the amoebae, as visualized by clear plaques corresponding to zones where actively feeding and replicating amoebae have phagocytized bacteria. In contrast, no plaques were formed with *B. cenocepacia* K56-2, demonstrating that wild-type K56-2 is resistant to *D. discoideum* predation (data not shown). To rule out the possibility that *B. cenocepacia* K56-2 does not support *Dictyostelium* growth, the ability of *D. discoideum* to grow on a thin lawn of *B. cenocepacia* K56-2 cells was tested by using low-nutrient plates (SM/50, SM/100) to limit bacterial growth. Clear

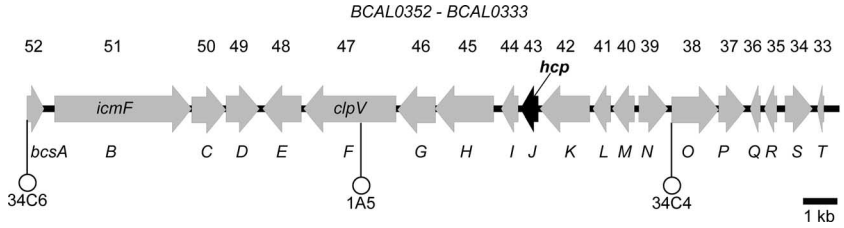

FIG. 5. Genetic map of the T6SS gene cluster. The location of the transposon in the 34C6, 1A5, and 34C4 mutants, which are attenuated for survival in the rat agar bead model (23), is indicated by white circles. This cluster has been designated the *bcs* cluster for *B. cenocepacia* survival. The location and direction of transcription of genes are represented by arrows. Locus tags assigned by the Sanger Center are shown above and the *bcs* annotation of the genes is shown below. The genes *icmF* (BCAL0351; *bcsB*), *clpV* (BCAL0347; *bcsF*), and *hcp* (BCAL0343; *bcsJ*), which are characteristic of T6SSs in other bacteria, are shown.

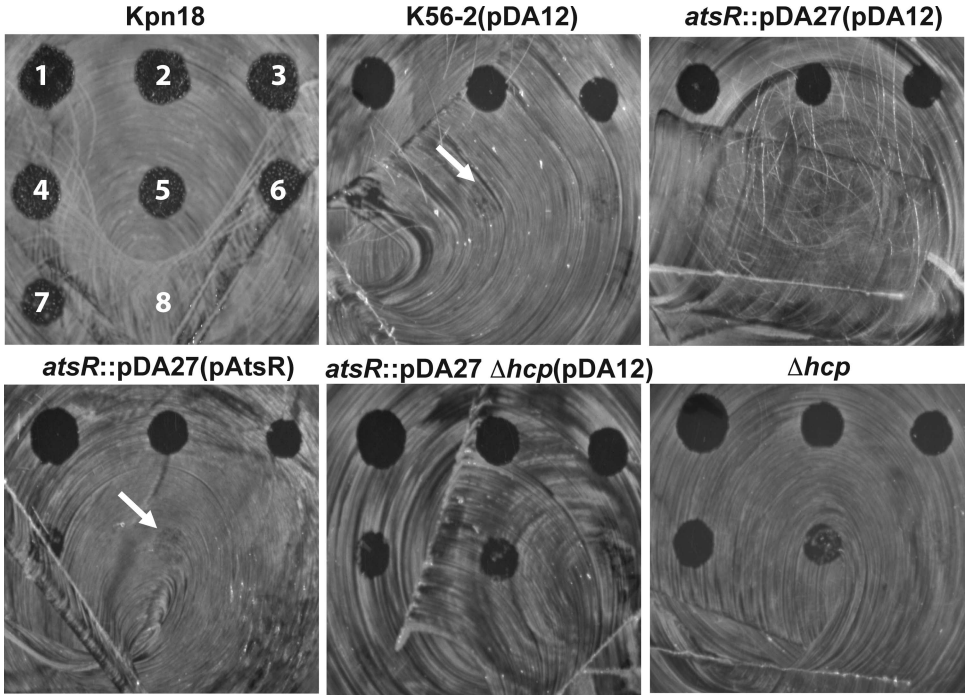

FIG. 6. Quantitative plaque assay. *D. discoideum* cells were applied as droplets onto a lawn of bacterial strains without plasmid or with the control vector pDA12 and pAtsR plasmids, as indicated in parentheses. *atsR* indicates DFA21; *atsR* Δ*hcp* indicates DFA28; Δ*hcp* indicates DFA27. The numbers of *Dictyostelium* cells applied were 50,000 (spot 1, as labeled for *K. pneumoniae* 18 [upper left]), 25,000 (spot 2), 12,500 (spot 3), 62,500 (spot 4), 3,125 (spot 5), 1,562 (spot 6), and 781 (spot 7); SorC buffer alone is shown for spot 8. After 3 days at 22°C, the ability of *Dictyostelium* cells to create plaques in the bacterial lawn was recorded. WT, wild type.

plaques were visualized after a few days, suggesting that low concentrations of *B. cenocepacia* K56-2 can support *D. discoideum* growth (data not shown).

The virulence of DFA21 relative to that of the parental strain was quantitatively characterized by spotting serial dilutions of amoeba cells on bacterial lawns (Fig. 6). This assay measures the lowest number of amoeba cells required for effective bacterial predation. The higher the number of amoebae required for bacterial killing, the higher is the ability of bacteria to resist predation. In the control experiment, *D. discoideum* formed clear plaques on the *K. pneumoniae* 18 lawn up to the lowest dilution tested, which contained 781 amoeba cells (Fig. 6). In contrast, *D. discoideum* at dilutions containing fewer than 3,125 amoebae did not form plaques on *B. cenocepacia* K56-2 (Fig. 6). On DFA21, 12,500 *Dictyostelium* cells was the lowest amount deposited on the plate leading to the formation of a visible plaque (Fig. 6), suggesting that *atsR* inactivation increases the resistance of this strain to predation either by avoiding amoeba killing or by inhibiting *Dictyostelium* growth. The introduction of pAtsR into DFA21 restored the susceptibility of this mutant to wild-type levels of amoeba predation. DFA27 and DFA28 mutants were even more susceptible to predation than wild-type K56-2, allowing the formation of clear plaques at dilutions containing 3,125 amoebae. Together, these results suggest that there is a correlation between Hcp secretion and resistance to *D. discoideum* predation.

To test whether secreted factors were at least in part responsible for the growth inhibition of *D. discoideum*, amoebae were incubated with HL5 medium or with filtered culture supernatants of *Staphylococcus aureus* RN6390 or *B. cenocepacia* K56-2 and DFA21 prior to plating on a *K. pneumoniae* 18 lawn. *S. aureus* RN6390 was used as a positive control of cytotoxicity, as this strain secretes an alpha-toxin that leads to rapid cell lysis (17). As expected, no plaques were formed when *Dictyostelium* cells were preincubated with *S. aureus* RN6390 culture supernatants. No significant difference in the numbers of plaques formed was observed when amoebae were preincubated with HL5 medium or with culture supernatants of DFA21 or *B. cenocepacia* K56-2 wild type (data not shown). Under the conditions tested, our results suggest that the growth inhibition of DFA21 and the parental strain toward *Dictyostelium* is not due to secreted effectors alone but may also require bacterium-amoeba contact.

The T6SS from *B. cenocepacia* K56-2 mediates actin rearrangements in mammalian macrophages. ANA-1 murine macrophages were used as a mammalian model system to investigate interactions between DFA21 and phagocytic cells. Morphological changes of ANA-1 macrophages were observed at 4 h postinfection with live DFA21 compared to K56-2 (Fig. 7). The macrophages displayed globular protrusions that included vacuoles and bacterium-containing vacuoles (Fig. 7; also see Fig. 9 below). The macrophages excluded the membrane-impermeant dye trypan blue, indicating that the cells retain their membrane integrity (data not shown). Heat-inactivated DFA21 did not induce protrusion formation, suggesting that it is an active process that requires metabolically active bacteria (data not shown).

To distinguish whether hyperadherence or Hcp hypersecre-

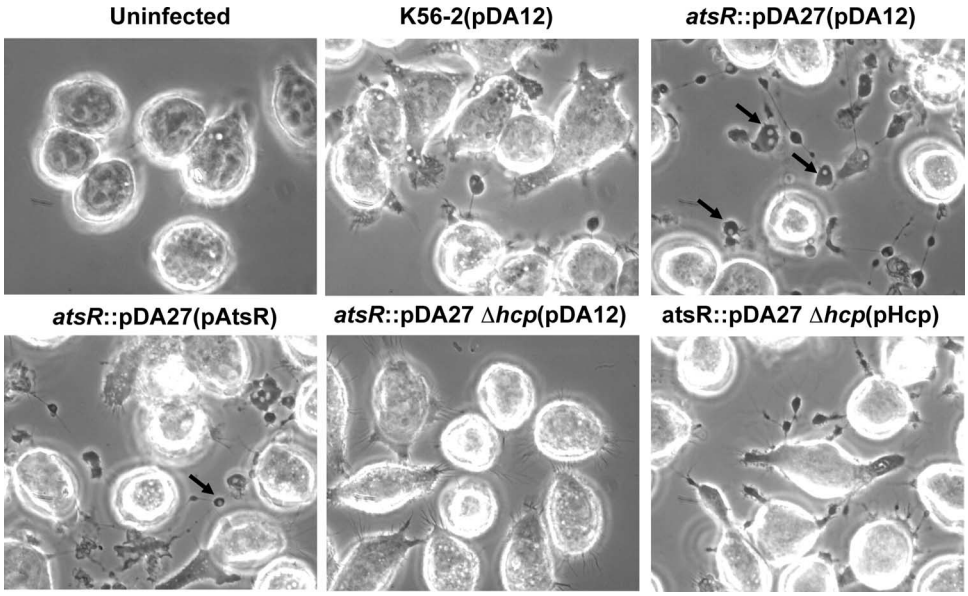

FIG. 7. Phase-contrast microscopy of infected ANA-1 macrophages. The infections were performed at an MOI of 50:1 for 4 h with parental and mutant strains containing pDA12, pAtsR, or pHcp as indicated in parentheses. *atsR* indicates DFA21; *atsR* Δ*hcp* indicates DFA28. Black arrows indicate vacuole-containing protrusions. WT, wild type.

tion was associated with the DFA21-mediated protrusions, ANA-1 cells were infected with DFA28, which has a hyperadherent phenotype (data not shown) but does not secrete Hcp (and potentially other T6SS effectors). DFA28 did not cause any detectable morphological changes in ANA-1 cells, whereas introduction of pHcp into DFA28 restored the ability of these bacteria to cause cellular protrusions. In addition, protrusions were still formed when ANA-1 cells were infected with DFA28(pAtsR), which secretes Hcp but does not have a hyperadherent phenotype, thus confirming that the formation of protrusions is mediated by the T6SS. Moreover, tissue culture medium supernatants from macrophages infected with DFA21 did not induce protrusions when added to wells containing uninfected ANA-1 cells, suggesting that the morphological changes require cell-to-cell contact between bacteria and macrophages (data not shown).

The morphological changes of the ANA-1 macrophages suggested an involvement of the cellular cytoskeleton. To elucidate in part the mechanism by which these protrusions were formed, ANA-1 cells were infected as previously described with DFA21 and filamentous actin was detected using phalloidin. In noninfected controls, filamentous actin was localized in the cytoplasm in a peripheral ring (data not shown; also see Fig. 9), while filamentous actin was significantly reorganized when the cells were infected with DFA21 (Fig. 8 and 9). Actin clumps could be found alone and in association with bacterium-containing vacuoles and also in the cytoplasmic protrusions (Fig. 8). In contrast, ANA-1 cells infected with DFA28 had a peripheral actin distribution very similar to that of uninfected cells (Fig. 8 and 9). Thus, DFA21 through the secretion of Hcp can induce actin rearrangements within macrophages, leading to the formation of cellular protrusions.

DISCUSSION

In this study, we have identified a putative sensor kinase-response regulator hybrid (AtsR) involved in the regulation of *B. cenocepacia* K56-2 virulence genes. AtsR contains one response regulator domain but lacks any DNA binding or Hpt (histidine phosphotransfer) domain, suggesting that other proteins are involved in the phosphorelay. The *atsR* gene is part of a three-gene operon together with BCAM0380 and BCAM0381, whose functions are unknown. We have preliminary evidence suggesting that BCAM0381 (which contains a response regulator domain as well as a helix-turn-helix binding motif) is part of the AtsR signaling pathway, but its position in the regulatory cascade is not yet elucidated (D. Aubert and M. Valvano, unpublished data).

We have determined that the inactivation of *atsR* in *B. cenocepacia* K56-2 leads to increased biofilm formation and adherence to polystyrene and lung epithelial cells. The genes that are required for biofilm maturation have been identified by transposon mutagenesis in *B. cepacia* H111 and can be divided into three main classes: genes encoding surface proteins (cable pili and adhesins), genes involved in the biogenesis and maintenance of outer membrane integrity, and genes that encode regulatory factors that affect *N*-acyl homoserine lactone production (21). Biofilm formation could be advantageous for *B. cenocepacia* in the CF lung environment in various ways. For example, bacteria could be protected from antibiotics and/or mediators of host defense (10). Also, increased adherence may facilitate epithelial cell invasion as well as the injection of bacterial molecules that are essential for virulence into the cell's cytoplasm. Consequently, biofilm formation plays an important role in the development of persistence leading to chronic inflammation and lung deterioration, which is the primary cause of mortality in CF patients. In the abiotic adhesion

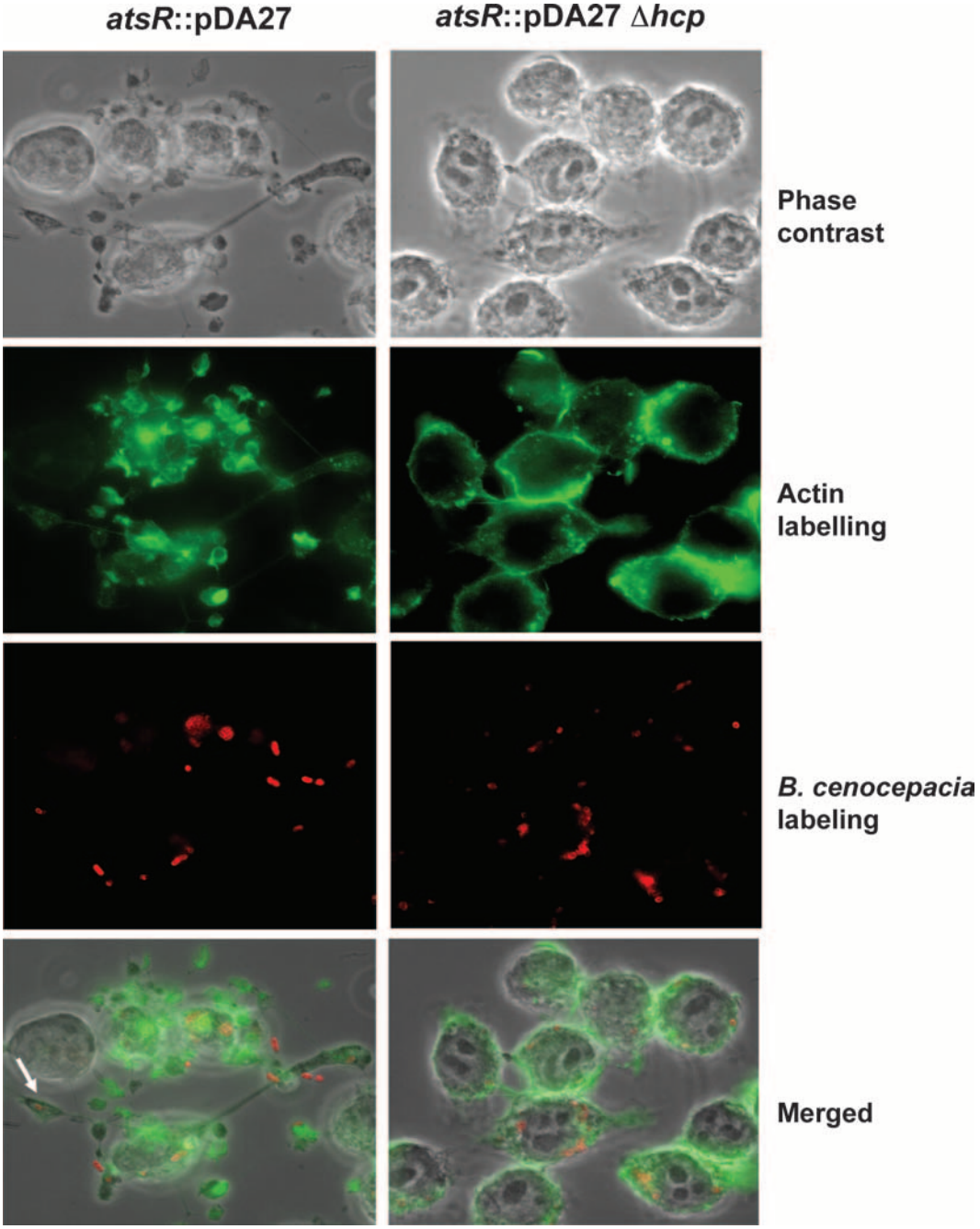

FIG. 8. Actin distribution of infected ANA-1 macrophages. Representative fluorescence micrographs of ANA-1 macrophages infected with strains DFA21 (shown as *atsR*) and DFA28 (shown as *atsR* Δ*hcp*) at an MOI of 50:1 for 4 h are shown. Green fluorescence denotes filamentous actin. Red fluorescence denotes individual *B. cenocepacia* bacteria. The white arrow indicates a protrusion with a bacterium-containing vacuole. WT, wild type.

assay, a centrifugation step was performed to enhance bacterial contact to the polystyrene surface. Since no centrifugation was performed in the adhesion experiments with A549 cells, this assay might reflect better the natural binding properties of *B. cenocepacia*. The molecular basis of the increased adherence in DFA21 is unknown. Studies of the *P. aeruginosa* Δ*retS* mutant suggest that hyperadherence is related to increased expression of two exopolysaccharide biosynthetic gene clusters (*pel* and *psl*). Microarray experiments, currently under way in our laboratory, will provide insight into the genes that are up- or downregulated in an *atsR* mutant background, as well as the genes involved in the hyperadherence phenotype of DFA21.

We determined that DFA21 overexpresses and hypersecretes an Hcp-like protein. In contrast to what was seen for *P. aeruginosa*, analysis of the sequenced genome of *B. cenocepacia* J2315 reveals that it encodes only one Hcp-like protein

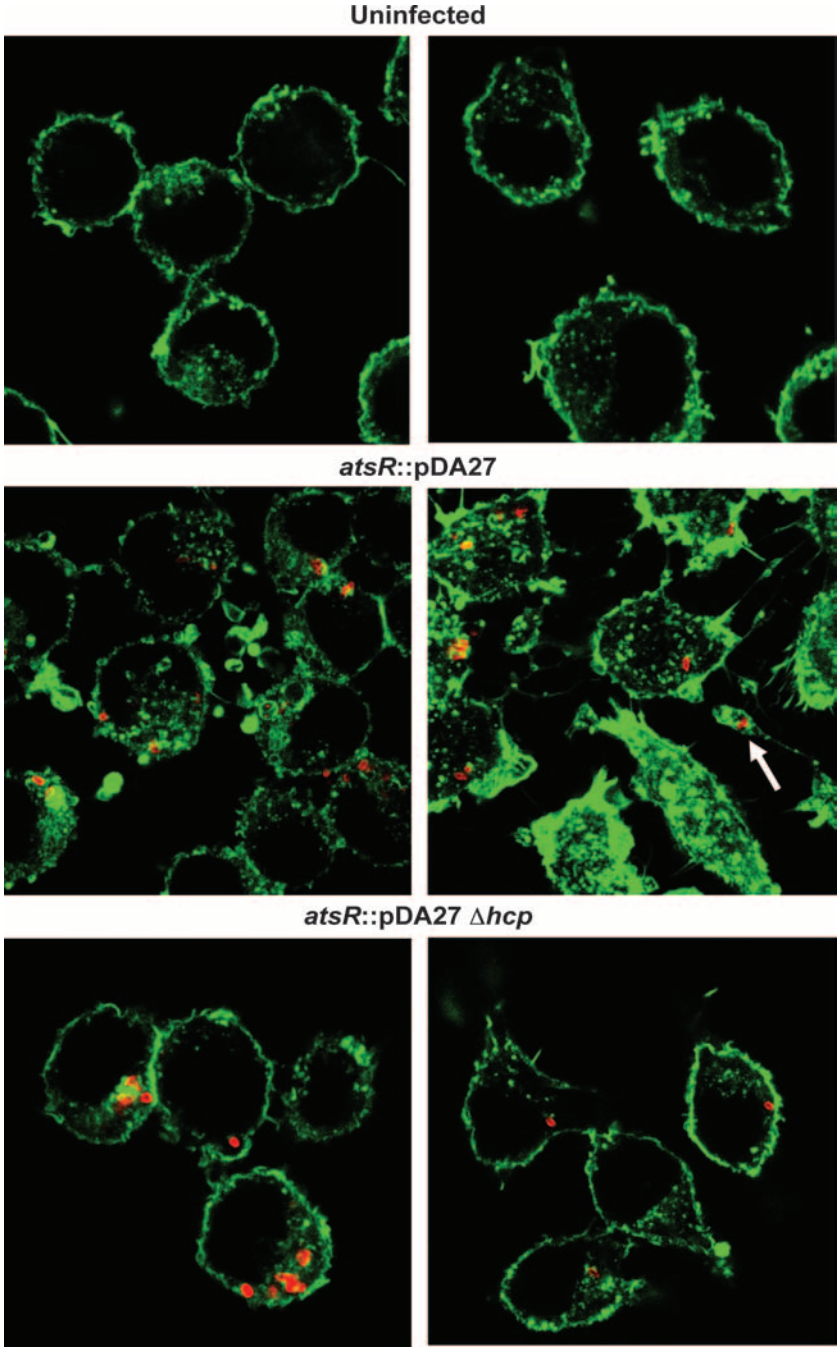

FIG. 9. Actin distribution of infected ANA-1 macrophages. Representative confocal images of uninfected ANA-1 macrophages or ANA-1 macrophages infected with DFA21 (indicated as *atsR*) or DFA28 (indicated as *atsR* Δ*hcp*) at an MOI of 50:1 for 4 h. Green fluorescence denotes filamentous actin. Red fluorescence denotes individual *B. cenocepacia* bacteria. The white arrow indicates a protrusion with a bacterium-containing vacuole.

(34). The *B. cenocepacia hcp* is likely part of an operon encoding other components of the T6SS, such as a ClpV-like chaperone (BCAL0347) shown in *P. aeruginosa* to be required for Hcp secretion (34). Thus, hypersecretion of Hcp in DFA21 is likely due to the overexpression of the entire T6SS rather than an overproduction of Hcp alone. Besides Hcp, other proteins are probably specifically secreted by the T6SS and remain to be identified. Orthologs of the genes encoding VgrG proteins from *V. cholerae* and *P. aeruginosa* are also found in the *B. cenocepacia* J2315 genome outside the T6SS locus identified in this study.

Interestingly, the majority of T6SSs studied to date have been discovered in mutant strains that overexpress the system (34, 40, 44), suggesting that T6SS is generally repressed in bacteria grown under laboratory conditions. Expression of the T6SS is tightly regulated and the mechanism of this regulation

involves two-component systems, transcriptional activators, and posttranslational regulation through threonine phosphorylation (34, 35, 40, 44). Upregulation of the T6SS by overexpression of the two-component system *virAG* in *Burkholderia mallei* (44) or by inactivation of *atsR* in *B. cenocepacia* is similar to the results observed with the global regulators RetS and LadS in *P. aeruginosa* (34, 54). RetS and LadS have reciprocal regulatory activities; therefore, RetS inactivation is equivalent to LadS overexpression and leads to the same phenotypes, including overexpression of the T6SS and increased biofilm formation. This reciprocal regulation controlling the expression of virulence factors is likely to occur in *Burkholderia* spp. and might be performed by the *virAG* and *atsR* homologs.

The *D. discoideum* plaque assays and macrophage infections performed in this study provide strong evidence that the T6SS plays an important role in *B. cenocepacia* K56-2 interactions with eukaryotic cells. From a previous screen in our laboratory for *B. cenocepacia* virulence genes, we identified three transposon insertion mutants (1A5, 34C4, 34C6) that were attenuated in the rat agar bead model of chronic lung infection (22). Further analysis indicated that these mutants had insertions within T6SS genes (Fig. 5 and data not shown), demonstrating that the T6SS is required for the virulence of *B. cenocepacia in vivo*.

D. discoideum and macrophage infection assays are relevant models for the study of *B. cenocepacia*. An extensive study performed in our laboratory showed that many clinical and environmental isolates of the BCC associated with CF persist within *Acanthamoeba* cells (32), suggesting that amoebae might be environmental reservoirs for BCC species. Electron micrographs have also shown that infected amoebae can release vacuoles containing bacteria that are sufficiently small to enter the human lower airway, potentially facilitating BCC colonization of the respiratory tract (32). *Acanthamoeba* and *D. discoideum* are remarkably similar to mammalian macrophages and our laboratory showed that BCC bacteria utilize a similar intracellular strategy to persist within amoebae and macrophages by delaying the phagosome-lysosome fusion (26, 27). The exact role of the T6SS in the resistance of *B. cenocepacia* K56-2 to *D. discoideum* predation is unknown. We noticed in our plaque assays that the size of the plaques formed by any of the *B. cenocepacia* strains tested (wild type or *hcp* mutant) remained unchanged even after 5 days (or more) of incubation, whereas plaques formed on a *K. pneumoniae* lawn continued to expand. In addition, the plaques formed on any *B. cenocepacia* lawn were characterized by the absence of fruiting bodies (a multicellular stage from *D. discoideum*), in contrast to lawns of *K. pneumoniae*, where fruiting bodies were abundant. These results suggest that *B. cenocepacia* resists *Dictyostelium* predation by actively killing the amoebae or inhibiting their growth and that virulence factors other than the T6SS may be involved.

Microarray analyses performed by others (16, 34) indicate that genes associated with chronic infections, such as biofilm-promoting genes, are upregulated in the *P. aeruginosa* Δ*retS* mutant, whereas genes associated with acute infections, such as the TTSS-encoding genes, are downregulated. Upregulation of the T6SS in the *P. aeruginosa retS* mutant suggests that this secretion system could be required for the development of chronic infection. Culture supernatants of the *atsR*::pDA27 mutant did not cause growth inhibition of *D. discoideum* or the morphological defects found upon bacterial infection of ANA-1 macrophages, suggesting that the T6SS requires bacterium-cell contact to exert its function. Our data clearly show the formation of cellular protrusions rich in actin that may include vacuoles or bacterium-containing vacuoles. It is currently unknown if formation of these protrusions involving actin rearrangements aid *B. cenocepacia* to escape from macrophages or delay the phagosome-lysosome fusion, an intracellular survival strategy known to be employed by *B. cenocepacia* (26). *B. cenocepacia* possesses other virulence factors, including a TTSS required for virulence in a murine infection model (53), two type IV secretion systems (12), extracellular proteases (5), hemolysin inducing degranulation and cell death in human phagocytes (23), and phospholipases, among others. Further investigations of the *B. cenocepacia* T6SS, including the molecular mechanism of secretion, are required for a better understanding of the role of this system in the persistence and intracellular survival of this bacterium and other related bacteria.

ACKNOWLEDGMENTS

We thank the members of our laboratory for helpful discussions, J. Parkhill for allowing us access to the draft annotation of *B. cenocepacia* J2315, D. Radzioch (McGill University, Department of Human Genetics, Montreal General Hospital Research Institute, Montreal, Quebec, Canada) for the gift of the ANA-1 cell line, P. Devreotes and the Dicty Stock Center for the gift of the *D. discoideum* AX3 strain, C. Y. Kang for the gift of the A549 cell line, D. E. Heinrichs for the gift of the *S. aureus* RN6390 strain, and K. E. Keith for help with confocal microscopy.

This work was supported in part by grants from the Canadian Cystic Fibrosis Foundation and the Canadian Institutes of Health Research (to M.A.V.). D.F.A. was supported by a Postdoctoral Fellowship from the Canadian Institutes of Health Research in partnership with the Association of Medical Microbiology and Infectious Disease Canada. R.S.F. was supported by a Graduate Student Fellowship from the Canadian Cystic Fibrosis Foundation. M.A.V. holds a Canada Research Chair in Infectious Diseases and Microbial Pathogenesis.

REFERENCES

1. **Bateman, A., L. Coin, R. Durbin, R. D. Finn, V. Hollich, S. Griffiths-Jones, A. Khanna, M. Marshall, S. Moxon, E. L. Sonnhammer, D. J. Studholme, C. Yeats, and S. R. Eddy.** 2004. The Pfam protein families database. Nucleic Acids Res. **32:**D138–D141.
2. **Chang, C., and R. C. Stewart.** 1998. The two-component system. Regulation of diverse signaling pathways in prokaryotes and eukaryotes. Plant Physiol. **117:**723–731.
3. **Coenye, T., and P. Vandamme.** 2003. Diversity and significance of *Burkholderia* species occupying diverse ecological niches. Environ. Microbiol. **5:**719–729.
4. **Cohen, S. N., A. C. Chang, and L. Hsu.** 1972. Nonchromosomal antibiotic resistance in bacteria: genetic transformation of *Escherichia coli* by R-factor DNA. Proc. Natl. Acad. Sci. USA **69:**2110–2114.
5. **Corbett, C. R., M. N. Burtnick, C. Kooi, D. E. Woods, and P. A. Sokol.** 2003. An extracellular zinc metalloprotease gene of *Burkholderia cepacia*. Microbiology **149:**2263–2271.
6. **Cosson, P., L. Zulianello, O. Join-Lambert, F. Faurisson, L. Gebbie, M. Benghezal, C. Van Delden, L. K. Curty, and T. Kohler.** 2002. *Pseudomonas aeruginosa* virulence analyzed in a *Dictyostelium discoideum* host system. J. Bacteriol. **184:**3027–3033.
7. **Cox, G. W., B. J. Mathieson, L. Gandino, E. Blasi, D. Radzioch, and L. Varesio.** 1989. Heterogeneity of hematopoietic cells immortalized by v-myc/v-raf recombinant retrovirus infection of bone marrow or fetal liver. J. Natl. Cancer Inst. **81:**1492–1496.
8. **Das, S., and K. Chaudhuri.** 2003. Identification of a unique IAHP (IcmF associated homologous proteins) cluster in *Vibrio cholerae* and other proteobacteria through in silico analysis. In Silico Biol. **3:**287–300.
9. **de Bruin, O. M., J. S. Ludu, and F. E. Nano.** 2007. The *Francisella* pathogenicity island protein IglA localizes to the bacterial cytoplasm and is needed for intracellular growth. BMC Microbiol. **7:**1.
10. **Desai, M., T. Buhler, P. H. Weller, and M. R. Brown.** 1998. Increasing resistance of planktonic and biofilm cultures of *Burkholderia cepacia* to ciprofloxacin and ceftazidime during exponential growth. J. Antimicrob. Chemother. **42:**153–160.
11. **Dower, W. J., J. F. Miller, and C. W. Ragsdale.** 1988. High efficiency transformation of *E. coli* by high voltage electroporation. Nucleic Acids Res. **16:**6127–6145.

12. **Engledow, A. S., E. G. Medrano, E. Mahenthiralingam, J. J. LiPuma, and C. F. Gonzalez.** 2004. Involvement of a plasmid-encoded type IV secretion system in the plant tissue watersoaking phenotype of *Burkholderia cenocepacia*. J. Bacteriol. **186:**6015–6024.
13. **Figurski, D. H., and D. R. Helinski.** 1979. Replication of an origin-containing derivative of plasmid RK2 dependent on a plasmid function provided in trans. Proc. Natl. Acad. Sci. USA **76:**1648–1652.
14. **Flannagan, R. S., D. Aubert, C. Kooi, P. A. Sokol, and M. A. Valvano.** 2007. *Burkholderia cenocepacia* requires a periplasmic HtrA protease for growth under thermal and osmotic stress and for survival in vivo. Infect. Immun. **75:**1679–1689.
15. **Flannagan, R. S., T. Linn, and M. A. Valvano.** A system for the construction of targeted unmarked gene deletions in the genus *Burkholderia*. Environ. Microbiol., in press.
16. **Goodman, A. L., B. Kulasekara, A. Rietsch, D. Boyd, R. S. Smith, and S. Lory.** 2004. A signaling network reciprocally regulates genes associated with acute infection and chronic persistence in *Pseudomonas aeruginosa*. Dev. Cell **7:**745–754.
17. **Gouaux, E.** 1998. Alpha-hemolysin from *Staphylococcus aureus*: an archetype of beta-barrel, channel-forming toxins. J. Struct. Biol. **121:**110–122.
18. **Govan, J. R., P. H. Brown, J. Maddison, C. J. Doherty, J. W. Nelson, M. Dodd, A. P. Greening, and A. K. Webb.** 1993. Evidence for transmission of *Pseudomonas cepacia* by social contact in cystic fibrosis. Lancet **342:**15–19.
19. **Govan, J. R., and V. Deretic.** 1996. Microbial pathogenesis in cystic fibrosis: mucoid *Pseudomonas aeruginosa* and *Burkholderia cepacia*. Microbiol. Rev. **60:**539–574.
20. **Hagele, S., R. Kohler, H. Merkert, M. Schleicher, J. Hacker, and M. Steinert.** 2000. *Dictyostelium discoideum*: a new host model system for intracellular pathogens of the genus *Legionella*. Cell. Microbiol. **2:**165–171.
21. **Huber, B., K. Riedel, M. Kothe, M. Givskov, S. Molin, and L. Eberl.** 2002. Genetic analysis of functions involved in the late stages of biofilm development in *Burkholderia cepacia* H111. Mol. Microbiol. **46:**411–426.
22. **Hunt, T. A., C. Kooi, P. A. Sokol, and M. A. Valvano.** 2004. Identification of *Burkholderia cenocepacia* genes required for bacterial survival in vivo. Infect. Immun. **72:**4010–4022.
23. **Hutchison, M. L., I. R. Poxton, and J. R. Govan.** 1998. *Burkholderia cepacia* produces a hemolysin that is capable of inducing apoptosis and degranulation of mammalian phagocytes. Infect. Immun. **66:**2033–2039.
24. **Isles, A., I. Maclusky, M. Corey, R. Gold, C. Prober, P. Fleming, and H. Levison.** 1984. *Pseudomonas cepacia* infection in cystic fibrosis: an emerging problem. J. Pediatr. **104:**206–210.
25. **Kolter, R., M. Inuzuka, and D. R. Helinski.** 1978. Trans-complementation-dependent replication of a low molecular weight origin fragment from plasmid R6K. Cell **15:**1199–1208.
26. **Lamothe, J., K. K. Huynh, S. Grinstein, and M. A. Valvano.** 2007. Intracellular survival of *Burkholderia cenocepacia* in macrophages is associated with a delay in the maturation of bacteria-containing vacuoles. Cell. Microbiol. **9:**40–53.
27. **Lamothe, J., S. Thyssen, and M. A. Valvano.** 2004. *Burkholderia cepacia* complex isolates survive intracellularly without replication within acidic vacuoles of *Acanthamoeba polyphaga*. Cell. Microbiol. **6:**1127–1138.
28. **Lefebre, M. D., and M. A. Valvano.** 2002. Construction and evaluation of plasmid vectors optimized for constitutive and regulated gene expression in *Burkholderia cepacia* complex isolates. Appl. Environ. Microbiol. **68:**5956–5964.
29. **Loutet, S. A., R. S. Flannagan, C. Kooi, P. A. Sokol, and M. A. Valvano.** 2006. A complete lipopolysaccharide inner core oligosaccharide is required for resistance of *Burkholderia cenocepacia* to antimicrobial peptides and bacterial survival in vivo. J. Bacteriol. **188:**2073–2080.
30. **Mahenthiralingam, E., T. Coenye, J. W. Chung, D. P. Speert, J. R. Govan, P. Taylor, and P. Vandamme.** 2000. Diagnostically and experimentally useful panel of strains from the *Burkholderia cepacia* complex. J. Clin. Microbiol. **38:**910–913.
31. **Mahenthiralingam, E., P. Vandamme, M. E. Campbell, D. A. Henry, A. M. Gravelle, L. T. Wong, A. G. Davidson, P. G. Wilcox, B. Nakielna, and D. P. Speert.** 2001. Infection with *Burkholderia cepacia* complex genomovars in patients with cystic fibrosis: virulent transmissible strains of genomovar III can replace *Burkholderia multivorans*. Clin. Infect. Dis. **33:**1469–1475.
32. **Marolda, C. L., B. Hauroder, M. A. John, R. Michel, and M. A. Valvano.** 1999. Intracellular survival and saprophytic growth of isolates from the *Burkholderia cepacia* complex in free-living amoebae. Microbiology **145:**1509–1517.
33. **Miller, V. L., and J. J. Mekalanos.** 1988. A novel suicide vector and its use in construction of insertion mutations: osmoregulation of outer membrane proteins and virulence determinants in *Vibrio cholerae* requires *toxR*. J. Bacteriol. **170:**2575–2583.
34. **Mougous, J. D., M. E. Cuff, S. Raunser, A. Shen, M. Zhou, C. A. Gifford, A. L. Goodman, G. Joachimiak, C. L. Ordonez, S. Lory, T. Walz, A. Joachimiak, and J. J. Mekalanos.** 2006. A virulence locus of *Pseudomonas aeruginosa* encodes a protein secretion apparatus. Science **312:**1526–1530.
35. **Mougous, J. D., C. A. Gifford, T. L. Ramsdell, and J. J. Mekalanos.** 2007. Threonine phosphorylation post-translationally regulates protein secretion in *Pseudomonas aeruginosa*. Nat. Cell Biol. **9:**797–803.
36. **Ortega, X., T. A. Hunt, S. Loutet, A. D. Vinion-Dubiel, A. Datta, B. Choudhury, J. B. Goldberg, R. Carlson, and M. A. Valvano.** 2005. Reconstitution of O-specific lipopolysaccharide expression in *Burkholderia cenocepacia* strain J2315, which is associated with transmissible infections in patients with cystic fibrosis. J. Bacteriol. **187:**1324–1333.
37. **O'Toole, G. A., and R. Kolter.** 1998. Flagellar and twitching motility are necessary for *Pseudomonas aeruginosa* biofilm development. Mol. Microbiol. **30:**295–304.
38. **Pukatzki, S., R. H. Kessin, and J. J. Mekalanos.** 2002. The human pathogen *Pseudomonas aeruginosa* utilizes conserved virulence pathways to infect the social amoeba *Dictyostelium discoideum*. Proc. Natl. Acad. Sci. USA **99:**3159–3164.
39. **Pukatzki, S., A. T. Ma, A. T. Revel, D. Sturtevant, and J. J. Mekalanos.** 2007. Type VI secretion system translocates a phage tail spike-like protein into target cells where it cross-links actin. Proc. Natl. Acad. Sci. USA **104:**15508–15513.
40. **Pukatzki, S., A. T. Ma, D. Sturtevant, B. Krastins, D. Sarracino, W. C. Nelson, J. F. Heidelberg, and J. J. Mekalanos.** 2006. Identification of a conserved bacterial protein secretion system in *Vibrio cholerae* using the *Dictyostelium* host model system. Proc. Natl. Acad. Sci. USA **103:**1528–1533.
41. **Rao, P. S., Y. Yamada, Y. P. Tan, and K. Y. Leung.** 2004. Use of proteomics to identify novel virulence determinants that are required for *Edwardsiella tarda* pathogenesis. Mol. Microbiol. **53:**573–586.
42. **Reik, R., T. Spilker, and J. J. Lipuma.** 2005. Distribution of *Burkholderia cepacia* complex species among isolates recovered from persons with or without cystic fibrosis. J. Clin. Microbiol. **43:**2926–2928.
43. **Sambrook, J., E. F. Fritsch, and T. Maniatis.** 1990. Molecular cloning: a laboratory manual, 2nd ed. Cold Spring Harbor Laboratory, Cold Spring Harbor, NY.
44. **Schell, M. A., R. L. Ulrich, W. J. Ribot, E. E. Brueggemann, H. B. Hines, D. Chen, L. Lipscomb, H. S. Kim, J. Mrazek, W. C. Nierman, and D. Deshazer.** 2007. Type VI secretion is a major virulence determinant in *Burkholderia mallei*. Mol. Microbiol. **64:**1466–1485.
45. **Sheahan, K. L., C. L. Cordero, and K. J. Satchell.** 2004. Identification of a domain within the multifunctional *Vibrio cholerae* RTX toxin that covalently cross-links actin. Proc. Natl. Acad. Sci. USA **101:**9798–9803.
46. **Smith, D. L., L. B. Gumery, E. G. Smith, D. E. Stableforth, M. E. Kaufmann, and T. L. Pitt.** 1993. Epidemic of *Pseudomonas cepacia* in an adult cystic fibrosis unit: evidence of person-to-person transmission. J. Clin. Microbiol. **31:**3017–3022.
47. **Solomon, J. M., A. Rupper, J. A. Cardelli, and R. R. Isberg.** 2000. Intracellular growth of *Legionella pneumophila* in *Dictyostelium discoideum*, a system for genetic analysis of host-pathogen interactions. Infect. Immun. **68:**2939–2947.
48. **Speert, D. P., D. Henry, P. Vandamme, M. Corey, and E. Mahenthiralingam.** 2002. Epidemiology of *Burkholderia cepacia* complex in patients with cystic fibrosis, Canada. Emerg. Infect. Dis. **8:**181–187.
49. **Steinert, M., and K. Heuner.** 2005. *Dictyostelium* as host model for pathogenesis. Cell. Microbiol. **7:**307–314.
50. **Stock, A. M., V. L. Robinson, and P. N. Goudreau.** 2000. Two-component signal transduction. Annu. Rev. Biochem. **69:**183–215.
51. **Suarez, G., J. C. Sierra, J. Sha, S. Wang, T. E. Erova, A. A. Fadl, S. M. Foltz, A. J. Horneman, and A. K. Chopra.** 24 October 2007. Molecular characterization of a functional type VI secretion system from a clinical isolate of *Aeromonas hydrophila*. Microb. Pathog. doi:10.1016/j.micpath.2007.10.005.
52. **Sussman, M.** 1987. Cultivation and synchronous morphogenesis of *Dictyostelium* under controlled experimental conditions. Methods Cell Biol. **28:**9–29.
53. **Tomich, M., A. Griffith, C. A. Herfst, J. L. Burns, and C. D. Mohr.** 2003. Attenuated virulence of a *Burkholderia cepacia* type III secretion mutant in a murine model of infection. Infect. Immun. **71:**1405–1415.
54. **Ventre, I., A. L. Goodman, I. Vallet-Gely, P. Vasseur, C. Soscia, S. Molin, S. Bleves, A. Lazdunski, S. Lory, and A. Filloux.** 2006. Multiple sensors control reciprocal expression of *Pseudomonas aeruginosa* regulatory RNA and virulence genes. Proc. Natl. Acad. Sci. USA **103:**171–176.
55. **West, A. H., and A. M. Stock.** 2001. Histidine kinases and response regulator proteins in two-component signaling systems. Trends Biochem. Sci. **26:**369–376.
56. **Williams, S. G., L. T. Varcoe, S. R. Attridge, and P. A. Manning.** 1996. *Vibrio cholerae* Hcp, a secreted protein coregulated with HlyA. Infect. Immun. **64:**283–289.
57. **Zheng, J., and K. Y. Leung.** 2007. Dissection of a type VI secretion system in *Edwardsiella tarda*. Mol. Microbiol. **66:**1192–1206.

Editor: J. N. Weiser